2007 IEEE International Conference on
Robotics and Automation
Roma, Italy, 10-14 April 2007

Time-Scaling Trajectories of Passive-Dynamic Bipedal Robots

Jonathan K. Holm*, Dongjun Lee**, and Mark W. Spong*

*Coordinated Science Laboratory
University of Illinois at Urbana-Champaign
1308 W. Main Street
Urbana, IL, 61801, USA

**Mechanical, Aerospace, &
Biomedical Engineering
University of Tennessee
1512 Middle Drive
Knoxville, TN 37996, USA

***Abstract*— This paper presents a control law that time-scales reference trajectories of dynamical systems, yielding arbitrary velocities in arbitrary time. It is shown that, for unforced (passive) reference trajectories, constant time-scaling results in a potential energy-shaping control. Application to walking trajectories of bipedal robots is shown, extending the use of the control beyond purely continuous dynamical systems to a class of hybrid dynamical systems with discontinuities that are linear in velocity. Two biped models are used to demonstrate the control law: for the compass-gait biped, we illustrate time-scaling of a passive reference trajectory; for the biped with a torso, we show time-scaling of a semi-passive reference trajectory.**

I. Introduction

Given a desired path for a robot, trajectory planning algorithms will sometimes specify motions that surpass the torque capabilities of one or more actuators. In such a case, actuators will saturate and the robot's trajectory will deviate from the nominal trajectory. Planning methods that account for dynamic limitations and generate physically feasible minimum-time trajectories were proposed almost simultaneously by Shin and McKay [13] and Bobrow, Dubowsky, and Gibson [1], which showed that strict minimum-time optimization results in bang-bang controllers, saturating at least one torque input at any given time. Modifications have since been presented by Shiller and Lu [12], Dahl and Nielsen [3], and others.

The passive-dynamic class of biped robots introduces two interesting variations on time-scaling. First, nominal trajectories for these machines are completely unforced; no actuation is necessary because the interplay of potential energy and energy dissipated through footsteps regulates the motion. None of the motors is used, much less saturated, in the passive case, allowing for great flexibility in time-scaling the unforced trajectory. Second, unlike the continuous dynamics of many manipulator tasks, the dynamics of biped robots is inherently hybrid due to the periodic foot-ground impacts which introduce velocity discontinuities between steps. The periodic discontinuties must be taken into account when time-scaling the biped trajectories.

We begin by developing the general time-scaling control law and then exploring the behavior of the control for a passive (unforced) reference trajectory. Specifically, we show that constant time-scaling of a passive trajectory results in a class of potential energy-shaping controls that has been studied by Licer, M'Sirdi, and Manamanni [8] and the first author [6].

The paper concludes with examples. We apply the time-scaling control law to two passive-dynamic bipeds: the compass-gait biped and a simple biped with torso. The hybrid dynamics of the biped robots is considered. Particular attention is paid to the discontinuity in velocities that occurs when a biped's food strike the ground. Simulation results are provided of each biped walking for a range of constant velocities, as well as transitioning from one velocity to another using a time-scaling function we develop.

II. Time-Scaling Control Law

A. Original Dynamics and Solution

Consider the following Lagrangian dynamics

$$M\big(q(t)\big)\ddot{q}(t) + C\big(q(t),\dot{q}(t)\big)\dot{q}(t) + G\big(q(t)\big) = \tau(t) \quad (1)$$

where M is the inertia matrix, C is the matrix of centrifugal and Coriolis terms, G is the gravity vector, and $\tau(t)$ is the vector of generalized input forces. Suppose that control input $\tau(t) = \tau_0(t)$ and initial conditions $\{q_0(0), \dot{q}_0(0)\}$ yield solution trajectory $q(t) = q_0(t)$ for $0 \le t \le T$ for some $T > 0$.

B. General Time-Scaling

Suppose that the dynamics (1) follows reference trajectory $q_0(t)$ w.r.t. scaled time $t' = \phi(t)$, where $\phi : \mathbb{R}^+ \to \mathbb{R}^+$ is a monotonic map s.t. $\frac{d}{dt}\phi(t) > 0$ for $0 \le t \le \phi^{-1}(T)$ and $\phi(0) = 0$. The scaled trajectory is

$$q_{sc}(t') = q_0\big(\phi(t)\big) = q_0(t') \quad (2)$$

where $0 \le t' \le \phi^{-1}(T)$. The scaled velocity and acceleration are given by

$$\dot{q}_{sc}(t') = \frac{\partial q_0(\phi)}{\partial \phi}\frac{d\phi}{dt} = \dot{q}_0(t')\dot{\phi} \quad (3)$$

$$\begin{aligned}\ddot{q}_{sc}(t') = &\ \tfrac{\partial \dot{q}_0(\phi)}{\partial \phi}\tfrac{d\phi}{dt}\dot{\phi} + \dot{q}_0(\phi)\tfrac{d\dot{\phi}}{dt} \\ = &\ \ddot{q}_0(t')\dot{\phi}^2 + \dot{q}_0(t')\ddot{\phi}.\end{aligned} \quad (4)$$

We rewrite dynamics (1) for the scaled trajectory $q_{sc}(t')$

$$\begin{aligned}M\big(q_{sc}(t')\big)\ddot{q}_{sc}(t') + C\big(q_{sc}(t'),\dot{q}_{sc}(t')\big)\dot{q}_{sc}(t') \\ +G\big(q_{sc}(t')\big) = \tau_{sc}(t').\end{aligned} \quad (5)$$

Substituting (2)-(4) into (5), we have

$$\begin{aligned}\tau_{sc}(t') &= M\big(q_0(t')\big)\big[\ddot{q}_0(t')\dot{\phi}^2 + \dot{q}_0(t')\ddot{\phi}\big]\ldots \\ &\quad +C\big(q_0(t'),\dot{q}_0(t')\dot{\phi}\big)\dot{q}_0(t')\dot{\phi} + G\big(q_0(t')\big) \\ &= \dot{\phi}^2\Big[M\big(q_0(t')\big)\ddot{q}_0(t') + C\big(q_0(t'),\dot{q}_0(t')\big)\dot{q}_0(t')\Big] \\ &\quad +M\big(q_0(t')\big)\dot{q}_0(t')\ddot{\phi} + G\big(q_0(t')\big) \\ &= \dot{\phi}^2\Big[\tau_0(t') - G(q_0(t'))\Big] + M\big(q_0(t')\big)\dot{q}_0(t')\ddot{\phi} \\ &\quad +G\big(q_0(t')\big)\end{aligned}$$

where the second equality follows from the fact that $C(q,\star)\star$ is quadratic in $\star$. Rearranging (1) and substituting into the last expression above, we have

$$\begin{aligned}\tau_{sc}(t') = \dot{\phi}^2\tau_0(t') + (1-\dot{\phi}^2)G(q_0(t') \\ +M\big(q_0(t')\big)\dot{q}_0(t')\ddot{\phi}.\end{aligned} \tag{6}$$

C. Special Case 1: Constant Time-Scaling

Consider the case of constant time-scaling for which the scaled time $t' = \phi(t)$ is given by $\phi(t) = \lambda t$ with $\lambda > 0$. Under this constraint, $\dot{\phi}(t) = \lambda$ and $\ddot{\phi}(t) = 0\ \forall t \geq 0$, simplifying the control law (6) to

$$\tau_{sc}(t') = \dot{\phi}^2\tau_0(t') + (1-\dot{\phi}^2)G(q_0(t') \tag{7}$$

and results in position, velocity, and acceleration that are multiples of the reference trajectory and powers of the time-scaling constant λ

$$\begin{aligned}q_{sc}(t') &= q_0(t') \\ \dot{q}_{sc}(t') &= \lambda\dot{q}_0(t') \\ \ddot{q}_{sc}(t') &= \lambda^2\ddot{q}_0(t')\end{aligned}$$

for $0 \leq t \leq \phi^{-1}(T) = \frac{T}{\lambda}$ with initial condition $\{q_{sc}(0),\dot{q}_{sc}(0)\} = \{q_0(0),\lambda\dot{q}_0(0)\}$.

D. Special Case 2: Passive Reference Trajectory

If, in addition to constant time-scaling, the reference trajectory is unforced ($\tau_0(t) = 0\ \forall t$) the control law (6) reduces to a potential energy-shaping control

$$\tau_{sc}(t') = (1-\dot{\phi}^2)G(q_0(t'))$$

which effectively "cancels" the effect of normal gravity $G(q_0)$ on the system dynamics (1) and substitutes the effect of scaled gravity $\dot{\phi}^2G(q_0)$.

III. Application One: Compass-Gait Biped

In this section we explore using time-scaling to alter the velocity of an unforced (passive) reference trajectory. In particular, we will examine the compass-gait biped robot which can walk down gentle slopes without any actuation [9], [2], [4]. A sketch of the compass-gait robot is provided in Fig. 1. The state consists of the two configuration variables (the angle of the stance leg w.r.t. the vertical θ_1 and the angle of the swing leg w.r.t. the vertical θ_2) and their derivatives.

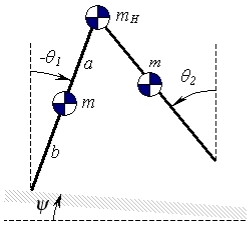

m	5kg
m_H	10kg
a	0.5m
b	0.5m
ℓ	$a+b$
g	9.8m/s^2

Fig. 1. The compass-gait biped and the parameter values used in our simulations.

A. Hybrid Dynamics

During the step, the behavior of the compass-gait biped is governed by the Lagrange dynamics (1) where $q(t) = [\theta_1(t),\theta_2(t)]^T$,

$$\begin{aligned}M &= \begin{bmatrix}(m_H+m)\ell^2+ma^2 & -m\ell b\cos(\theta_1-\theta_2)\\ -m\ell b\cos(\theta_1-\theta_2) & mb^2\end{bmatrix}, \\ C &= \begin{bmatrix}0 & -m\ell b\sin(\theta_1-\theta_2)\dot{\theta}_2\\ m\ell b\sin(\theta_1-\theta_2)\dot{\theta}_1 & 0\end{bmatrix}, \\ G &= g\begin{bmatrix}-(m_H\ell+ma+m\ell)\sin(\theta_1)\\ mb\sin(\theta_2)\end{bmatrix},\end{aligned}$$

and g is the acceleration due to gravity.

Between each step, the Lagrange dynamics is interrupted when the tip of the swinging leg contacts the walking surface while moving in the downward direction, i.e. when

$$y_{tip}(t) = \ell[\cos(\theta_1+\psi) - \cos(\theta_2+\psi)] = 0 \tag{8}$$

and

$$\dot{y}_{tip}(t) = \ell[\sin(\theta_2+\psi)\dot{\theta}_2 - \sin(\theta_1+\psi)\dot{\theta}_1] < 0 \tag{9}$$

where ψ is the slope of the walking surface. The compass-gait biped has a problem of the swing leg scuffing the ground as it swings past the stance leg. In practice, this scuffing has been avoided adding actuators to slightly retract the tip of the swing leg as it passes the stance leg or by having the biped walk on stepping stones. In simulation, we avoid scuffing by ignoring conditions (8) and (9) whenever the swing leg is behind the stance leg, i.e. when $\theta_1 > \theta_2$.

We make the following assumptions about the surface contact event:

1) the impact is perfectly plastic (no bounce occurs)
2) support is instantaneously transferred from the stance leg to the swing leg
3) the legs do not slip along the ground during the impact.

Under these assumptions, the impact results in an instantaneous change in angular velocities [7] while the angles of the legs remain unchanged $q(t^+) = q(t^-)$. In the previous expressions, t^- and t^+ denote the instants before and after the impact event, respectively.

For a biped composed of n-links in an open kinematic chain and subject to the three impact assumptions above, the instantaneous change in angular velocities at impact can be written as a linear map of pre-impact to post-impact velocities

$$\dot{q}(t^+) = h\big(q(t^-)\big)\dot{q}(t^-). \tag{10}$$

The linear mapping $h(q(t^-))$ can be found by applying the law of conservation of angular momentum. For the compass-gait biped, the map is given by

$$h(q(t^-)) = \begin{bmatrix} h_{11}^+ & h_{12}^+ \\ h_{21}^+ & h_{22}^+ \end{bmatrix}^{-1} \begin{bmatrix} h_{11}^- & h_{12}^- \\ h_{21}^- & h_{22}^- \end{bmatrix}$$

where

$$\begin{aligned} h_{11}^+ &= m\ell(\ell - b\cos(\theta_1^- - \theta_2^-)) + ma^2 + m_H\ell^2, \\ h_{12}^+ &= mb(b - \ell\cos(\theta_1^- - \theta_2^-)), \\ h_{21}^+ &= -mb\ell\cos(\theta_1^- - \theta_2^-),\ h_{22}^+ = mb^2 \\ h_{11}^- &= -mab + (m_H\ell^2 + 2ma\ell)\cos(\theta_1^- - \theta_2^-), \\ h_{12}^- &= h_{21}^- = -mab,\ h_{22}^- = 0. \end{aligned}$$

For a detailed derivation, please consult Appendix A of [4].

B. Passive Limit Cycle

A passive limit cycle exists for zero input torque $\tau_0(t) = 0$ on a slope of $\psi = 0.052$rad. We choose our initial condition to be the point on the limit cycle corresponding to the start of a step, given by

$$\{q_0(0), \dot{q}_0(0)\} = \{0.2187, -0.3234, -1.0918, -0.3772\}$$

Integrating (1), we monitor (8) and (9) until the instant prior to ground impact $t^- = 0.735\text{s} \equiv T$. This trajectory from $0 \le t \le T$ will be our reference trajectory $q_0(t)$.

C. Effect of the Impact Event

The linear map $h\big(q(t^-)\big)$ between velocities at the end and beginning of each step is completely determined by the configuration at the end of the step $q(t^-)$. We have chosen our reference trajectory so that the terminating configuration $q_0(T)$ is the configuration of the end of the step $q_0(t^-)$. Since the final configuration of the time-scaled trajectory $q_{sc}\big(\phi^{-1}(T)\big) = q_0(T)$ is invariant under our control law, the map

$$h\Big(q_{sc}\big(\phi^{-1}(T)\big)\Big) = h\big(q_0(T)\big)$$

is constant regardless of what time-scaling function $\phi(t)$ we choose.

For the reference trajectory $\{q_0(t), \dot{q}_0(t)\}$, we have

$$\dot{q}_0(t^+) = h\big(q_0(t^-)\big)\dot{q}_0(t^-)$$

and, since the trajectory is a limit cycle, the post-impact final velocity is equivalent to the initial velocity $\dot{q}_0(t^+) = \dot{q}_0(0)$. Under constant time-scaling $\phi(t) = \lambda t$, we have $\dot{q}_{sc}(t') = \lambda\dot{q}_0(t')$. Consequently,

$$\begin{aligned} \dot{q}_{sc}(t^+) = \lambda \cdot \dot{q}_0(t^+) &= \lambda \cdot h\big(q_0(t^-)\big)\dot{q}_0(t^-) \\ &= h\big(q_0(t^-)\big) \cdot \lambda\dot{q}_0(t^-) \\ &= h\big(q_{sc}(t^-)\big)\dot{q}_{sc}(t^-) \end{aligned}$$

and

$$\dot{q}_{sc}(t^+) = \lambda\dot{q}_0(t^+) = \lambda\dot{q}_0(0) = \lambda\dot{q}_{sc}(0),$$

so the impact event scales the impact velocities linearly by the constant λ, matching the scaling of the rest of the trajectory and effectively "stretching" the entire limit cycle.

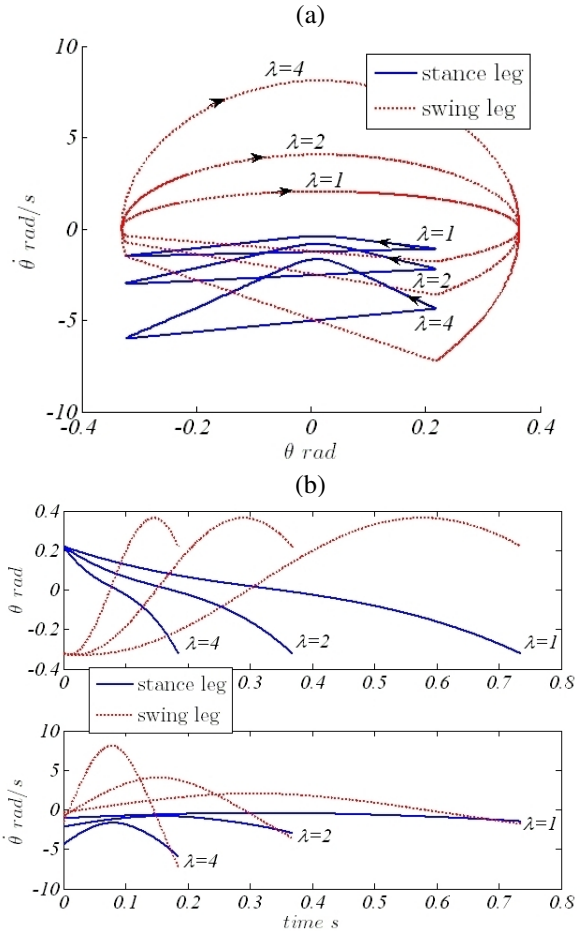

Fig. 2. Compass gait biped under constant time-scaling control $\phi(t) = \lambda t$ with various values of parameter λ. (a) scaled limit cycles (b) scaled system trajectories.

Under variable time-scaling $\phi(t)$, a similar expression holds. However, since the scaling is nonuniform, the post-impact final velocity $\dot{q}_{sc}(t^+)$ is *not* the same as the initial velocity of the trajectory $\dot{q}_{sc}(0)$. Instead, the final velocity serves as the initial condition of a new limit cycle with a velocity different from the original.

D. Constant Time-Scaling

We first consider the case of constant time-scaling given by $\phi(t) = \lambda t$ with $\lambda > 0$. Since we are making use of an unforced reference trajectory, the control law reduces to the potential energy-shaping control (7) which relates the velocity of the biped to a constant multiple of the gravity vector. McMahon [10] and McGeer [9] noted this quadratic relationship between walking speed and the acceleration of gravity. More recently, Licer et al. [8] and Holm [6] have explored this relationship with various robot models.

Fig. 2 shows limit cycles and time-scaled trajectories for various values of λ. We see from the figures that the initial and final values of the configuration variables θ_1, θ_2 are identical while the velocities $\dot{\theta}_1, \dot{\theta}_2$ vary with selection of the parameter λ.

E. Varying Time-Scaling

In the previous section, we showed that constant time-scaling yields limit cycles with velocity of our choice. However, constant time-scaling requires that the initial condition be on the desired limit cycle . Nonconstant time-scaling allows for beginning on a limit cycle of one velocity and ending on a limit cycle of a different velocity. In this section, we develop a nonconstant time-scaling function to move between limit cycles in a single step.

Previous work accomplished varying time-scaling by gradually changing parameter λ of the constant time-scaling control law (7), see Saimek and Li's work with swimming machines [11] and the first author's work with passive-dynamic bipeds [6]. This approach is imprecise, requiring changes in λ to be sufficiently slow to prevent the trajectory from exiting the controller's basin of attraction. Here, our general time-scaling control law (6) is based on arbitrary time-scaling function $\phi(t)$; this formulation affords the flexibility of designing $\phi(t)$ to change the time scaling of the system in arbitrary time.

Consider the task of transitioning from a limit cycle described by constant time-scaling function $\phi_1(t) = \lambda_1 t$ and another limit cycle described by $\phi_2(t) = \lambda_2 t$. Clearly, $\dot{\phi}_i(t) = \lambda_i$ for each of these limit cycles. To move from one to the other, we construct a time-scaling function $\phi_\Delta(t)$ whose derivative is equal to λ_1 at the beginning of the step and equal to λ_2 at the end of the step. That is,

$$\begin{aligned} \phi_\Delta(0) &= 0 \qquad & \phi_\Delta(t_F) &= T \\ \dot{\phi}_\Delta(0) &= \lambda_1 \qquad & \dot{\phi}_\Delta(t_F) &= \lambda_2 \end{aligned}$$

where $t_F = \phi^{-1}(T)$ is the desired time (in seconds) of the end ground impact, which we are free to choose provided $\frac{d}{dt}\phi_\Delta(t) > 0$ for $0 \le t \le t_F$. These four conditions are satisfied by the cubic polynomial given by

$$\begin{aligned} \phi_\Delta(t) = \lambda_1 t + \left(\tfrac{3T}{t_F^2} - \tfrac{2\lambda_1+\lambda_2}{t_F}\right) t^2 \\ + \left(-\tfrac{2T}{t_F^3} + \tfrac{\lambda_1+\lambda_2}{t_F^2}\right) t^3. \end{aligned} \tag{11}$$

Fig. 3(a) is a phase portrait of the compass gait biped under our time-scaling control transitioning from the passive limit cycle described by $\lambda_1 = 1$ to a limit cycle described by $\lambda_2 = 2$ with varying time-scaling $\phi_\Delta(t)$ and transition time $t_F = 0.5$s. Fig. 3(b) shows the trajectories of the system as it moves from the passive limit cycle ($\lambda_1 = 1$) limit cycle to the $\lambda_2 = 2$ limit cycle.

IV. Application Two: Biped with Torso

We now employ time-scaling to change the velocity of a system with an actuated reference trajectory. Our sample application is a biped robot with a torso [5]. We have seen that a biped robot without a torso can walk without actuation, but the the presence of a torso requires active control to keep the torso upright during walking. The biped is illustrated in Fig. 4. The state consists of three configuration variables $\theta_1, \theta_2, \theta_T$–the angles of the stance leg, swing leg, and torso link w.r.t. the vertical–and their derivatives.

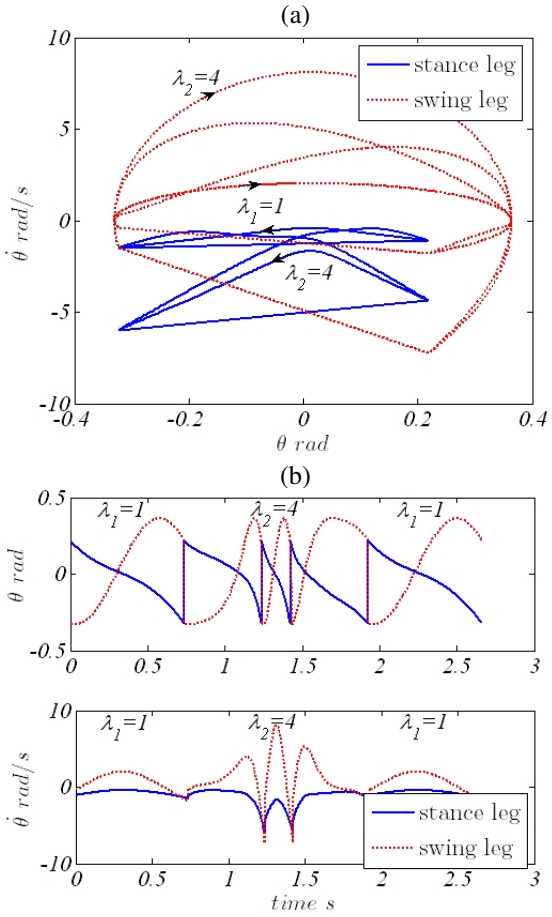

Fig. 3. Compass gait biped under varying time-scaling; here it is shown transitioning from the original limit cycle ($\lambda_1 = 1$) to a time-scaled limit cycle described by $\lambda_2 = 2$. (a) Phase portrait of swing and stance legs and (b) system trajectories.

A. Hybrid Dynamics

During the step, the behavior of the biped with torso is governed by the Lagrange dynamics (1) where $q(t) = [\theta_1(t), \theta_2(t), \theta_T(t)]^T$,

$$M = \begin{bmatrix} (\frac{5}{4}m + m_H + m_T)r^2 & -\frac{1}{2}mr^2c_{12} & m_T r\ell c_{1T} \\ -\frac{1}{2}mr^2c_{12} & \frac{1}{4}mr^2 & 0 \\ m_T r\ell c_{13} & 0 & m_T\ell^2 \end{bmatrix},$$

$$C = \begin{bmatrix} 0 & -\frac{1}{2}mr^2 s_{12}\dot{\theta}_2 & m_T r\ell s_{1T}\dot{\theta}_T \\ \frac{1}{2}mr^2 s_{12}\dot{\theta}_1 & 0 & 0 \\ -m_T r\ell s_{1T}\dot{\theta}_1 & 0 & 0 \end{bmatrix},$$

$$G = g\begin{bmatrix} -(m_H + \frac{3}{2}m + m_T)r\sin(\theta_1) \\ \frac{1}{2}mr\sin(\theta_2) \\ -m_T\ell\sin(\theta_T) \end{bmatrix},$$

$s_{ij} = \sin(\theta_i - \theta_j)$, $c_{ij} = \cos(\theta_i - \theta_j)$, and g is the acceleration due to gravity.

As with the compass-gait biped, the continuous Lagrange dynamics of the biped with torso is interrupted when the tip of the swinging leg contacts the walking surface. We make the same assumptions as before about the surface contact event, which leads us to another linear mapping of pre- and post-impact velocities that is dependent only on the

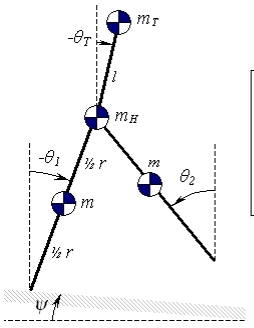

m	5kg
m_H	10kg
m_t	10kg
r	1m
ℓ	0.5m
g	9.8m/s^2

Fig. 4. The biped with torso and the parameter values used in our simulations.

configuration of the robot immediately prior to the impact

$$\dot{q}(t^+) = h\big(q(t^-)\big)\dot{q}(t^-).$$

There are multiple methods for deriving the impact map $h\big(q(t^-)\big)$; we follow the derivation provided in [5]. The method begins by adding cartesian coordinates z_1, z_2 of the tip of the stance leg to the vector of generalized coordinates, resulting in $q_e = [\theta_1, \theta_2, \theta_t, z_1, z_2]^T$. We rederive the Lagrange dynamic equations in these new coordinates and add an instantaneous term that models the impact forces as an impulse

$$M_e\big(q_e\big)\ddot{q_e} + C_e\big(q_e, \dot{q}_e\big)\dot{q}_e + G_e\big(q_e\big) = \tau_e + \delta F. \qquad (12)$$

Integrating both sides of (12) from time t^- to t^+ yields

$$M(q_e(t^-))(\dot{q}_e^+ - \dot{q}_e^-) = F \qquad (13)$$

where F is the vector of forces due to the impact. Inertia matrix M_e in (12) is symmetric with entries on and above the diagonal given by

$$\begin{aligned}
M_{e(1,1)} &= \tfrac{1}{4}(5m + 4m_H + 4m_T)r^2,\\
M_{e(1,4)} &= -\tfrac{1}{2}(3m + 2m_H + 2m_T)r\cos(\theta_1),\\
M_{e(1,5)} &= -\tfrac{1}{2}(3m + 2m_H + 2m_T)r\sin(\theta_1),\\
M_{e(4,4)} &= M_{e(5,5)} = 2m + m_H + m_T.
\end{aligned}$$

$$\begin{aligned}
M_{e(1,2)} &= -\tfrac{1}{2}mr^2c_{12}, & M_{e(1,3)} &= m_Tr\ell c_{1t},\\
M_{e(2,2)} &= \tfrac{1}{4}mr^2, & M_{e(2,3)} &= 0,\\
M_{e(2,4)} &= \tfrac{1}{2}mr\cos(\theta_2), & M_{e(2,5)} &= \tfrac{1}{2}mr\sin(\theta_2),\\
M_{e(3,3)} &= m_T\ell^2, & M_{e(4,5)} &= 0,\\
M_{e(3,4)} &= -m_T\ell\cos(\theta_t), & M_{e(3,5)} &= -m_T\ell\sin(\theta_t).
\end{aligned}$$

Since the pivot point of the stance leg is assumed to detach without interaction the instant after impact, the impact forces F act only on the tip of swing leg. Define Γ_e to be the cartesian coordinates of the tip of the swing leg

$$\Gamma_e = \begin{bmatrix} z_1 - r\sin(\theta_1) + r\sin(\theta_2) \\ z_2 + r\cos(\theta_1) - r\cos(\theta_2) \end{bmatrix}.$$

The impact forces F on the swing leg may be written as

$$F = -\Big(\frac{\partial\Gamma_e}{\partial q_e}\Big)^T \begin{bmatrix} F_{tang} \\ F_{norm} \end{bmatrix} \qquad (14)$$

where F_{tang} and F_{norm} are the tangential and normal forces, respectively, acting on the tip of the swing leg. Substituting (14) into (13) yields a set of five equations in seven unknowns. An additional two equations come as a consequence of the impact assumptions. The slipless, perfectly plastic impact indicates that the swinging leg does not rebound at impact. We can write the constraint of no rebound at impact as

$$\frac{d\Gamma_e}{dt}(t^+) = \frac{\partial\Gamma_e}{\partial q_e}\dot{q}_e^+ = 0. \qquad (15)$$

Combining (13)-(15) into a single matrix expression, the impact velocity map $\dot{q}^+ = h\big(q(t^-)\big)\dot{q}^-$ is found by solving

$$\begin{bmatrix} \dot{q}_e^+ \\ \big(F\big) \end{bmatrix} = \begin{bmatrix} M_e(q_e) & -\Big(\frac{\partial\Gamma_e}{\partial q_e}\Big)^T \\ \Big(\frac{\partial\Gamma_e}{\partial q_e}\Big) & 0 \end{bmatrix}^{-1} \begin{bmatrix} M_e(q_e)\dot{q}_e^- \\ 0 \end{bmatrix}$$

for $\dot{q}_e^+$, noting that $\dot{q}^+$ is simply the first three elements of $\dot{q}_e^+$.

B. Torso Balancing Control

The biped's torso behaves as an inherently unstable inverted pendulum. While a passive limit cycle exists for the legs, some active control is required to keep the torso upright. We use the simple PD control

$$\tau_0(t) = \begin{bmatrix} 0 \\ 0 \\ -k_p\left(\theta_T(t) - \theta_T^d\right) - k_d\dot{\theta}_T(t) \end{bmatrix} \qquad (16)$$

and choose desired torso angle $\theta_T^d = -\psi$. Thus, were the biped walking on level ground, the torso would be held vertical.

The PD control (16) is analogous to a spring and damper, which could effectively replace the control law and render the biped with torso completely passive.

C. Semi-Passive Limit Cycle

A limit cycle exists for the biped with knees on a slope of $\psi = 0.052$rad and PD control (13) with high gains $k_p = 700$ and $k_d = 200$. We again choose the initial conditon of our reference trajectory to be the point on the limit cycle corresponding to the start of a step, given by

$$\{q_0(0), \dot{q}_0(0)\} = \begin{array}{l}\{0.2358, -0.3405, -0.0441,\\ -0.8585, -0.0307, -0.9951\}\end{array}$$

Integrating (1), we monitor (8) and (9) until the instant prior to ground impact $t^- = 0.7624\text{s} \equiv T$. This trajectory from $0 \le t \le T$ will be the reference trajectory $q_0(t)$.

D. Constant Time-Scaling

We first consider the case of constant time-scaling given by $\phi(t) = \lambda t$ with $\lambda > 0$. Fig. 5 shows limit cycles for various values of λ. We see from the figures that the initial and final values of the configuration variables $\theta_1, \theta_2, \theta_T$ are identical while the velocities $\dot{\theta}_1, \dot{\theta}_2, \dot{\theta}_T$ vary with selection of the parameter λ.

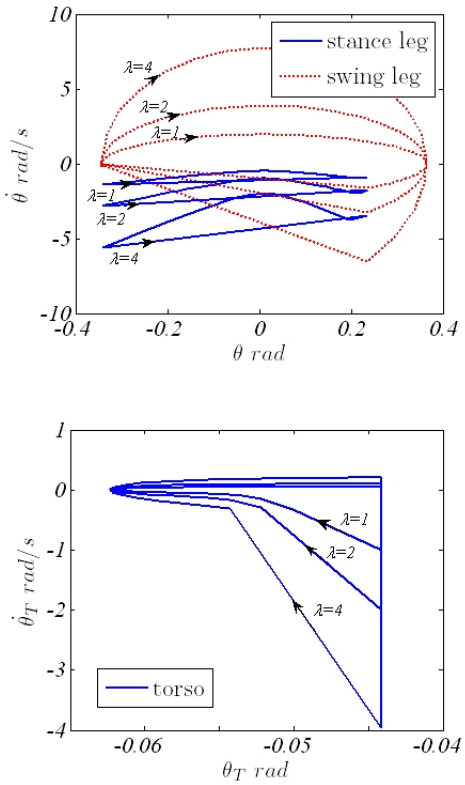

Fig. 5. Limit cycles of the biped with knees under constant time-scaling control $\phi(t) = \lambda t$ with various values of parameter λ.

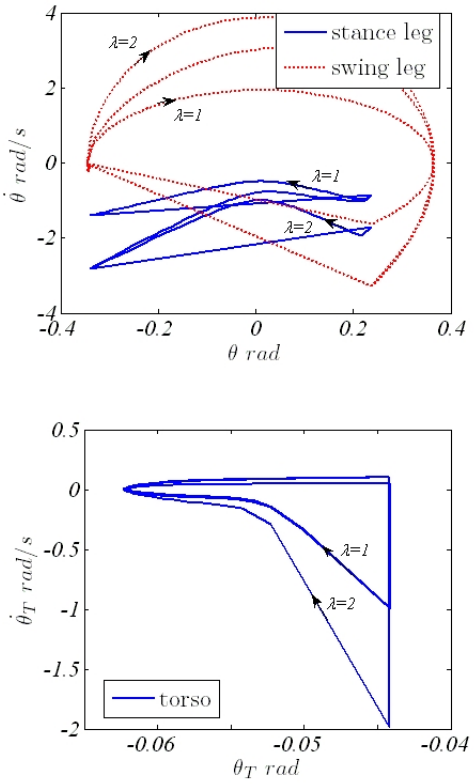

Fig. 6. Biped with knees under varying time-scaling; here it is shown transitioning from the original limit cycle ($\lambda_1 = 1$) to a time-scaled limit cycle described by $\lambda_2 = 2$.

E. Varying Time-Scaling

We again consider the task of moving from a limit cycle described by constant time-scaling function $\phi_1(t) = \lambda_1 t$ and another limit cycle described by $\phi_2(t) = \lambda_2 t$ using the time-scaling fuction (11). Fig. 6 is a phase portrait of the biped with torso under our time-scaling control transitioning from the limit cycle described by $\lambda_1 = 1$ to one described by $\lambda_2 = 4$ in one step with varying time-scaling $\phi_\Delta(t)$ and transition time $t_F = 0.5$s.

V. Conclusions

We have illustrated constant and variable time-scaling for the specific example of the compass-gait biped, yet the control result is very general. Indeed, these results hold for *all* continuous dynamical systems satisfying (1) and all hybrid systems obeying (1) and with instantaneous discontinuities that are linear in the velocities (10). In the special case of bipedal robots, bipeds modeled as open kinematic chains with impacts obeying the three assumptions stated above will result in hybrid systems to which these time-scaling techniques can be applied. These include bipeds with knees and bipeds with knees and torsos.

References

[1] J.E. Bobrow, S. Dubowsky, and J.S. Gibson, "Time-optimal control of robotic manipulators along specified paths," *Int. J. Robotics Research*, vol. 4, no. 3, 1985, pp. 3-17.

[2] S. Collins, A. Ruina, R. Tedrake, and M. Wisse, "Efficient bipedal robots based on passive dynamic walkers," *Science*, vol. 307, 2005, pp. 1082-1085.

[3] O. Dahl and L. Nielsen, "Torque-limited path following by on-line trajectory time scaling," *IEEE Trans. Robotics & Automation*, vol. 6, no. 5, 1990, pp. 554-561.

[4] A Goswami, B Thuilot, and B. Espiau, "Compass-like biped robot Part I: Stability and bifurcation of passive gaits," Institut National de Recherche en Informatique et en Automatique (INRIA), Tech. Rep. 2996, 1996.

[5] J.W. Grizzle, G. Abba, and F. Plestan, "Asymptotically stable walking for biped robots: analysis via systems with impulse effects," *IEEE Trans. Automatic Control*, vol. 46, no. 1, Jan 2001, pp.51-64.

[6] J.K. Holm, "Control of passive dynamic robots using artificial potential energy fields," Univ. Illinois Urbana-Champaign, M.S. thesis, 2005.

[7] Y. Hurmuzlu and G. Moskowitz, "The role of impact in the stability of bipedal locomotion," *Dynamics and Stability of Systems*, vol. 1, no. 3, 1986, pp. 217-234.

[8] O. Licer, N.K. M'Sirdi, and N. Manamanni, "Stable periodic gaits of n-link biped robot in three dimensional space," *IFAC Symp. Robot Control*, Bologna, Italy, 2006. *In press.*

[9] T. McGeer, "Passive dynamic walking," *Int. J. Robotics Research*, vol. 9, no. 2, 1990, pp. 62-82.

[10] T. McMahon, "Mechanics of locomotion," *Int. J. Robotics Research*, vol. 3, no. 2, 1984, pp. 4-28.

[11] S. Saimek and P.Y. Li, "Motion planning and control of a swimming machine," *Int. J. Robotics Research*, vol. 23, 2004, pp. 27-54.

[12] Z. Shiller and H.H. Lu, "Computation of path constrained time optimal motions with dynamic singularities," *ASME J. Dyn. Sys., Meas., & Cont.*, vol. 114, 1992, pp. 34-40.

[13] K.G. Shin and N.D. McKay, "Minimum-time control of robotic manipulators with geometric path constraints," *IEEE Trans. Aut. Control*, vol. 30, no. 6, 1985, pp. 531-541.